International Journal of Heat and Mass Transfer 51 (2008) 5823–5827

Contents lists available at ScienceDirect

International Journal of Heat and Mass Transfer

journal homepage: www.elsevier.com/locate/ijhmt

Kinetics of water adsorption on loose grains of SWS-1L under isobaric stages of adsorption heat pumps: The effect of residual air

I.S. Glaznev, Yu.I. Aristov *

Boreskov Institute of Catalysis, Pr. Lavrentieva, 5, Novosibirsk 630090, Russia

ARTICLE INFO

Article history:
Received 19 February 2008
Received in revised form 14 March 2008
Available online 4 July 2008

Keywords:
Adsorption kinetics
Non-adsorbable gas
Adsorption heat pumps
Selective water sorbent
Silica gel

ABSTRACT

In this paper we studied the effect of a non-adsorbable gas (air) on kinetics of water adsorption on loose grains of the composite adsorbent SWS-1L (silica modified by calcium chloride) (grain size 0.8–0.9 and 1.4–1.6 mm). The adsorbent grains were placed on the surface of isothermal metal plate at $T = 60$ °C and equilibrated with the mixture of water vapor at $P_{H_2O} = 10.3$ mbar and air at a certain partial pressure P_A. After that the metal plate was subjected to a temperature drop down to 35 °C at almost constant pressure over the grains. Reduction of the adsorption rate was revealed even at the partial pressure of residual air P_A as low as 0.06 mbar. At $P_A > 0.4$ mbar the kinetic curves were near-exponential and the characteristic adsorption time τ did not depend on the grain size and increased as $\tau = \tau_0 + AP_A$, where $A = 700 \pm 50$ s/mbar. Desorption stage was less affected by the residual air. The specific cooling power generated during the isobaric adsorption stage was estimated as a function of the residual air pressure.

1. Introduction

Adsorption of water vapor is an important part of many industrial systems such as steam power plants, seawater desalination units, absorption and adsorption heat pumps, etc. Adsorption of pure vapor on a single adsorbent grain is generally controlled by surface or/and intraparticle heat and mass transfer resistance, and it has been studied in detail. The water adsorption (condensation) from binary mixtures produces an extra heat and mass transfer resistance from the gas phase side. This resistance may become very large if one of the components is a non-adsorbable (non-condensable) gas [1]. In practice such a gas can present inside an evacuated equipment: air due to leakage or desorption, hydrogen due to corrosion, etc. The slowing down of the adsorption process was assumed to be caused by the effective gas sweeping to the surface where it accumulates as a gas-rich layer [2,3]. The transfer of vapor to the surface may then become controlled by the process of diffusion through this layer which is relatively slow compared with adsorption process controlled by surface and intraparticle resistances.

Many authors have revealed the reduction of condensation rate in the presence of non-condensable gases [4–7]. It was found that depending on concentration, a half percent of air in steam can reduce the heat transfer in absorption heat pumps by 50% [8]. An absorption reduction of about 300% was reported at a non-absorbable gas concentration of 5% [9]. A 6-fold reduction in the coefficient of performance of the entire absorption machine in the air presence in concentration of only 2% was predicted in [10].

The influence of a non-adsorbable gas on the rate of water adsorption has not been purely studied so far. In [11] authors revealed the reduction of heat transfer in a granulated adsorbent layer in the presence of residual air. It was supposed that this effect can significantly reduce the performance of an adsorption heat pump (AHP). In [12] it was stated that "as little as 1–2% non-condensing gases such as air can "poison" two-phase heat transfer, reducing evaporator and condenser heat rate by 50%", although no justification was presented.

The aim of this paper was the experimental investigation of the water adsorption dynamics during an isobaric adsorption stage of an AHP cycle, which is the most sensitive to the presence of non-adsorbable gas. We used a new dynamic approach that was proposed in [13,14]. It allows obtaining the uptake curve for an adsorbent located on a metal holder subjected to a fast temperature drop which initiates the water adsorption much as in adsorption heat pumps. The kinetics of adsorption was studied for loose grains of SWS-1L under the following boundary conditions: the initial pressure of water vapor 10.3 mbar, the initial temperature 60 °C and the temperature drop was 25 °C so that the final temperature of the metal holder was set at 35 °C. These conditions are typical for adsorption stage of AHP with the evaporator temperature 10 °C and minimal adsorber temperature 35 °C.

The measurements were carried out for composite SWS-1L formed by a dry impregnation of silica KSK with hygroscopic $CaCl_2$ [15]. Salt confinement to the pores was suggested to increase the water sorption capacity of a common mesoporous silica for

* Corresponding author. Tel./fax: +7 383 330 9573.
E-mail address: aristov@catalysis.ru (Yu.I. Aristov).

0017-9310/$ - see front matter © 2008 Elsevier Ltd. All rights reserved.
doi:10.1016/j.ijheatmasstransfer.2008.04.061

Nomenclature

A	coefficient (s/mbar)
AHP	adsorption heat pump
d	differential operator (−)
h_{fg}	latent heat of water vaporization (2478 kJ/kg)
M	molar weight (0.018 kg/mol)
m	weight of adsorbed water (kg)
m_{ads}	weight of dry adsorbent (kg)
P	pressure (mbar)
R	gas constant (8.31 kJ/kg K^{-1})
r	grain radius (mm)
t	time (s)
T	temperature (K)
V	volume (m^3), valve
3WV	three-way valve
W	specific power (W/kg)

Greek symbols

Δ	difference operator (−)
τ	characteristic time (s)

Subscripts

0	initial value (at $t = 0$ or at $P_A = 0$ mbar)
A	ambient air
H_2O	water vapor
ev	evaporator
f	final value
max	maximum
MC	measuring cell
t	instantaneous value at time t
VV	vapor vessel

application in adsorption heat pumps [16]. Indeed, SWS-1L was successfully tested in a prototype of water chilling unit ensuring its quite efficient performance [17].

2. Experimental apparatus, procedure and materials

2.1. Apparatus

The general design of the experimental setup was similar to that described in [13]. It contained three main compartments: the measuring cell (volume $V_{MC} = 0.14 \times 10^{-3}$ m^3), the vapor vessel ($V_{VV} = 30.5 \times 10^{-3}$ m^3) and the evaporator with liquid water (Fig. 1). Loose adsorbent grains were placed on an isothermal surface of the metal holder. Its temperature can be adjusted with the accuracy of ±0.1 °C using a heat carrier circuit coupled by a three-way valve (3WV) either to circulating thermal bath 1 or 2.

The temperature of the constant volume vapor vessel as well as all connecting pipelines was maintained at 60 ± 0.5 °C by using the air bath oven. Water vapor was generated by the evaporator with a cooling jacket. The evaporator temperature was managed by circulating thermal bath 2 through the valve V_{ev}. This temperature unambiguously set the vapor pressure which was measured by an absolute pressure transducer MKS Baratron® type 626A (accuracy ±0.01 mbar).

Three-way valves were installed into the heat carrier loop to leap the metal plate temperature. By rotating the 3WV to the reverse position, the heat carrier flows from bath 1 and 2 could be switched and, thus, initiating either desorption or adsorption process.

2.2. The tested sorbent

The tested adsorbent SWS-1L was prepared by a silica KSK impregnation with a saturated aqueous solution of $CaCl_2$ at $T = 25$ °C. The synthesis procedure was described in [15]. The salt content amounted to 33.7 wt.% (dry base). The average pore diameter of SWS-1L amounted to 15 nm. Two grain sizes were selected: 0.8–0.9 and 1.4–1.6 mm. Typical weight of the dry sample was 0.420–0.425 g that corresponded to a one layer of loose grains covering the metal plate.

2.3. Experimental procedure

Typical experimental run was as follows. The dry sorbent was heated to the starting temperature of the isobaric adsorption stage $T_0 = 60$ °C and evacuated for 2 h using a vacuum pump (valves V_{MC}, V_2, V_3 are opened, V_A and V_1 are closed). Then the vapor vessel was filled with water vapor by its connecting to the evaporator and the starting pressure for the adsorption process P_{ev} ($T = 10$ °C) = 12.4 mbar was set (V_1 was open, V_2 and V_{MC} were closed). Then, the measuring cell was connected with the vapor vessel (V_{MC} and V_3 were open, V_1 and V_2 were closed) and the sample was equilibrated with water vapor for 2 h. The air was let inside the setup as a non-adsorbable gas through a fine control needle valve V_A. Valves V_{MC} and V_1 were closed, so that the air additive could be uniquely identified by the pressure increment ΔP. Before to start the kinetic measurements, we were waiting up for reaching a homogeneous distribution of air for 1 h.

To initiate the adsorption process the metal holder was cooled down to $T_f = 35$ °C by turning 3WV (V_{MC} was open). It resulted in reducing the vapor pressure over the adsorbent, which did not exceed 2.0–2.5 mbar, so that the process can be considered as quasi-isobaric. Small reduction of the vapor pressure during the adsorption stage can be a case for real AHPs with undersized evaporators which can not maintain the vapor pressure constant. After reaching the adsorption equilibrium the reverse temperature leap was performed to initiate the desorption run.

Data of the pressure evolution $P(t)$ required for calculating the water uptake $\Delta m_{H_2O}(t)$ were recorded each 1 s by a data acquisition system. The uptake was calculated as ([13])

$$\Delta m_{H_2O} = M \cdot \frac{\Delta P (V_{MC} + V_{VV})}{RT} \quad (1)$$

A detailed analysis for the accumulated error in estimating the absolute water loading showed a maximum value of $\pm 10^{-3}$ kg/kg that leads to the accuracy of the differential water loading equal to ±1.5%.

3. Results and discussion

Typical evolution of the temperature of the metal plate, the vapor pressure over the sample and the water uptake is shown in Fig. 2. After initiating the holder cooling, its temperature reached the final temperature T_f within app. 1 min (Fig. 2a), while the pressure reduction was slower and completed within some ten minutes (Fig. 2b). As a first approximation, the adsorption took place at constant temperature of the holder equal to its final temperature as it was considered in the model described in [14].

Adsorption of a pure vapor (the pressure of residual air $P_A \leqslant 10^{-2}$ mbar) was faster for smaller adsorbent grains (Fig. 3). The shape of these kinetic curves was near-exponential over the range $0 \div 80\%$ of the final uptake. The characteristic times $\tau_{0.5}$

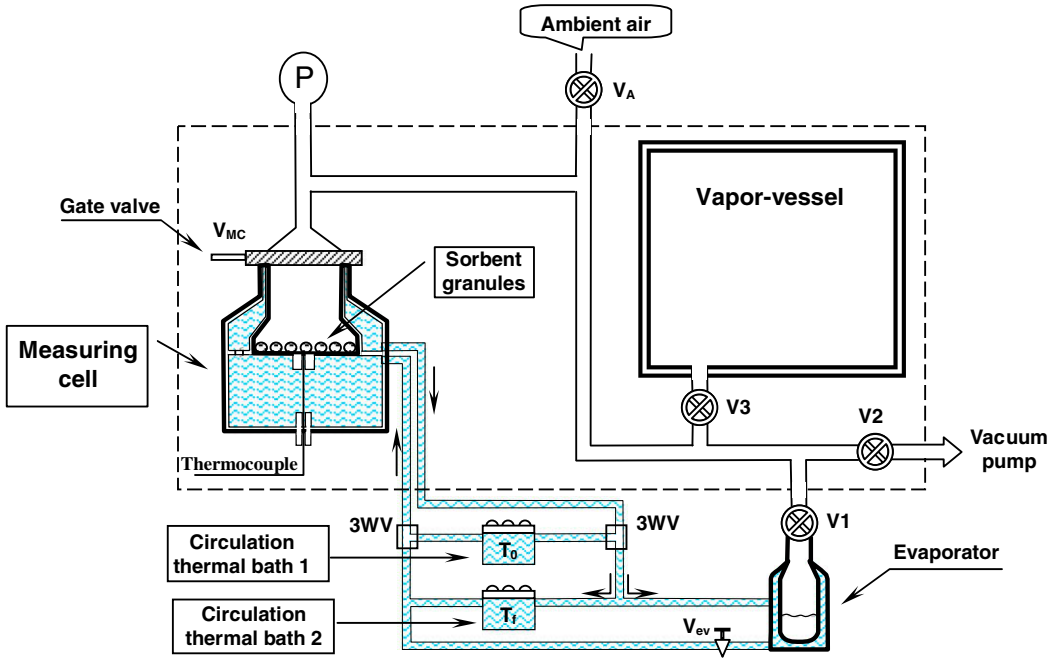

Fig. 1. Schematic diagram of the kinetic setup.

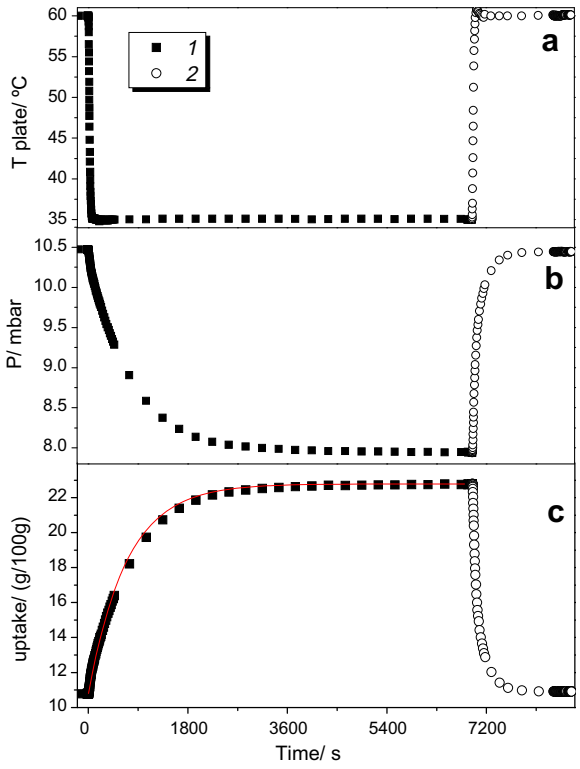

Fig. 2. The temperature evolution of metal plate (a), the pressure over the sample (b) and the water uptake (c) for cooling (1) and heating (2) runs for grains 0.8–0.9 mm at $P_A = 0.4$ mbar. The solid line is an exponential approximation $m_t = m_0 + (m_f - m_0) \cdot (1 - \exp(-t/\tau))$.

and $\tau_{0.8}$ corresponding to 50% and 80% of the final uptake were 2 ÷ 15 min. (Fig. 3). The ratio $\tau_{0.5}^{1.5\ mm}/\tau_{0.5}^{0.85\ mm} \approx \tau_{0.8}^{1.5\ mm}/\tau_{0.8}^{0.85\ mm} \approx 2.5$ was close to $(r^{1.5\ mm}/r^{0.85\ mm})^2 = 3.1$ that may indicate a significant contribution of the intraparticle vapor diffusion and/or of the heat emission from the grain surface to the total adsorption rate.

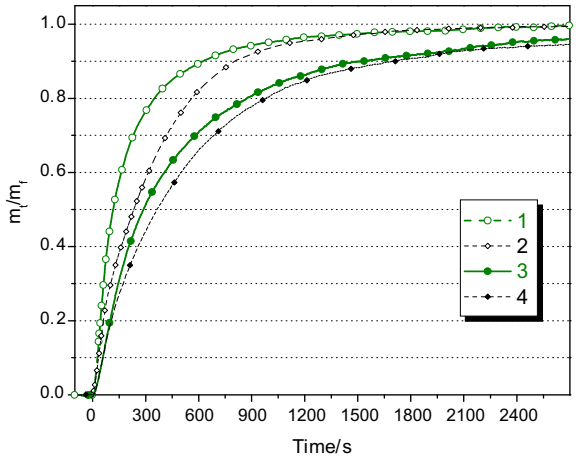

Fig. 3. The inhibition of adsorption rate in the presence of air: fraction 0.8–0.9 mm (P_A: *1*–0 mbar, *2*–0.06 mbar) and fraction 1.4–1.6 mm (3–0 mbar, 4–0.06 mbar). $P_0(H_2O) = 10.3$ mbar.

We found that the presence of air at the partial pressure as low as 0.06 mbar can visibly decrease the rate of adsorption (Fig. 3). It was especially significant at the intermediate uptakes $0.3 < m_t/m_f < 0.9$ while at $m_t/m_f < 0.2$ and $m_t/m_f > 0.95$ no influence of residual air on the shape of the kinetic curves was revealed (Fig. 3). According to [2,3], the reduction of the adsorption rate can be caused by the Stephan flux which effectively sweeps air to the grain surface where it accumulates as a gas-rich layer. Coupled transfers through this layer occur by mass diffusion and heat conduction. At higher air pressure the adsorption in the presence of air was slower at any uptake, at $P_A \geqslant 1.0$ mbar the kinetic curves being coincident for the grains of 0.8–0.9 and 1.4–1.6 mm size (Fig. 4). Hence, the adsorption process is likely to be controlled by the external mass transfer resistance caused by the slow diffusion of water vapor through the air-rich layer accumulated near the external surface of the grains. This non-stationary layer can also affects the heat transfer from the external grain surface.

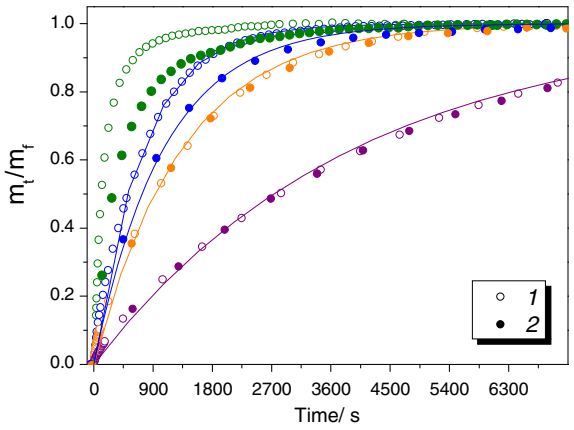

Fig. 4. The dimensionless uptake curves at different partial pressure of air (in order P_A = 0, 0.4, 1 and 4.7 mbar from left to right). Fraction 0.8–0.9 mm (1) and 1.4–1.6 mm (2). Symbols – experiment, lines – approximation by the function $m_t = m_0 + (m_f - m_0) \cdot (1 - \exp(-t/\tau))$.

Moreover, air can also accumulates inside the grain pores so that the combined effects of all these impacts on the adsorption rate should be a subject of detailed mathematical modeling.

At $P_A \geqslant 0.4$ mbar the kinetic curves were near-exponential over the all range of uptake so that $m_t = m_0 + (m_f - m_0) \cdot (1 - \exp(-t/\tau))$. At $P_A \geqslant 1$ mbar the characteristic time of adsorption increased as $\tau = \tau_0 + AP_A$, where $A = 700 \pm 50$ s/mbar for the both grain sizes (Fig. 5).

Desorption stage was less affected by the residual air (Figs. 2 and 6) because the air-rich layer did not form on this case. The desorption rate was limited by the intraparticle vapor diffusion or the dissipation of adsorption heat from the grain external surface.

The average specific power $W(t)$ (W/kg) consumed in the evaporator during the water adsorption stage is a key parameter of AHP. It defines the necessary amount of adsorbent and the size of the unit. For exponential adsorption kinetics this power can be calculated as

$$W(t) = h_{fg} \frac{dm}{dt} \cdot \frac{1}{m_{ads}} = h_{fg} \frac{m_f - m_0}{m_{ads}} \cdot \frac{e^{-t/\tau}}{\tau} = W_{max} \cdot e^{-t/\tau} \qquad (2)$$

Herein, h_{fg} is the latent heat of evaporation of liquid water taken as 2478 kJ/kg, $W_{max} = h_{fg}(m_f - m_0)/(m_{ads} \cdot \tau)$ is the maximum specific power which is released at $t \to 0$. Thus, W^0_{max} was equal to 0.57 and 1.54 kW/kg under the fixed initial conditions (P_{H_2O} = 10.3 mbar, P_A = 0 mbar, $T = 60 \to 35$ °C) for SWS-1L grains of 1.4–1.6 mm and 0.8–0.9 mm size, respectively. As evident from Eq. (2), the average power $W(t)$ decreases in the course of the adsorption process, therefore it is reasonable to stop the isobaric adsorption when the uptake reaches 80–90% of the equilibrium one. As $\tau_{0.8} = -\tau \cdot \ln(0.2)$, the average power $W_{0.8} = \frac{1}{\tau_{0.8}} \int_0^{\tau_{0.8}} W(t)dt \approx 0.5 W_{max}$. This still gives the specific power which is quite suitable for AHP, hence, one layer of loose grains can be considered as an acceptable configuration for modern AHPs as it was suggested in [18]. Since the characteristic adsorption time slows down in the presence of air, it results in the appropriate decreasing of the both W_{max} and $W_{0.8}$ (Fig. 5).

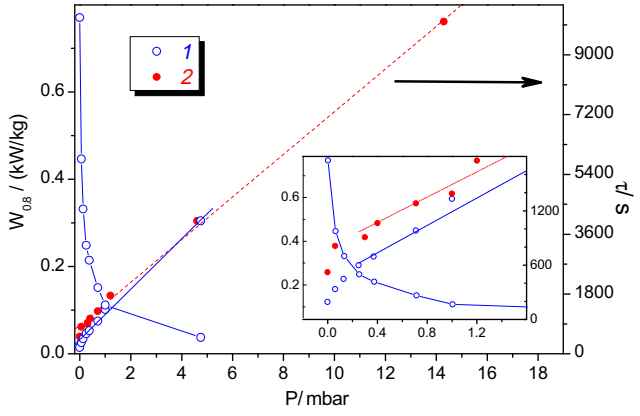

Fig. 5. Characteristic time τ and specific power $W_{0.8}$ vs. the air pressure for grains of 0.8–0.9 mm (1) and 1.4–1.6 mm size (2). Lines – linear approximations τ[s] = 870 + 642 $^*P$[mbar] for grains 1.4–1.6 mm (dotted line) and τ[s] = 434 + 756 $^*P$[mbar] for grains 0.8–0.9 mm (solid line).

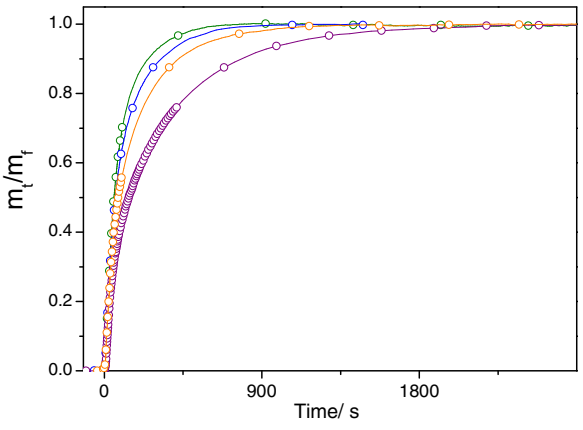

Fig. 6. Dimensionless desorption uptake curves at different partial pressure of air (in order P_A = 0, 0.4, 1 and 4.7 mbar from left to right). Fraction 0.8–0.9 mm.

For instance, for SWS-1L grains of 0.8–0.9 mm size the specific power $W_{0.8}$ reduces almost by 3.5 times in the presence of just 0.5 mbar of air (Fig. 5) that is similar to the strong air effect reported in [8]. As the influence of residual gases is essential, AHP should be equipped with a purge system to remove the gases originated from leaks or corrosion processes inside the machine. In such a system the gases are separated in a trap, whereas the vapor is returned to the machine, e.g. as it is organized in absorption heat chillers [19].

4. Conclusions

Thus, a wealth of reliable data on the kinetics of water vapor adsorption on the loose grains of SWS-1L has been measured under real conditions of AHP. The data can be used to assess the influence of residual air as well as to predict the performance at the isobaric adsorption stage of AHPs. Reduction of the rate of water adsorption was revealed even at the partial pressure of residual air P_A as low as 0.06 mbar. At $P_A > 0.4$ mbar the kinetic curves were near-exponential and at $P_A \geqslant 1$ mbar the characteristic adsorption time τ did not depend on grain size and increased as $\tau = \tau_0 + AP_A$, where $A = 700 \pm 50$ s/mbar. The specific cooling power generated during the isobaric adsorption stage was estimated as a function of the residual air pressure.

Acknowledgment

The authors thank the Russian Foundation for Basic Researches (projects 08-08-00808 and 08-08-90016) for partial financial support.

References

[1] D.M. Ruthven, Principles of Adsorption and Adsorption Processes, Wiley, New York, 1984.
[2] W. Nusselt, Surface condensation of water vapor, Z. Ver. Deut. Ing. 60 (1916) 541–546.

[3] D.A. Frank-Kamenetskiy, Diffusion and Heat Transfer in Chemical Kinetics, Nauka, Moscow, 1967.
[4] J.W. Rose, Condensation of a vapour in the presence of a non-condensing gas, Int. J. Heat Mass Transfer 12 (1969) 233–247.
[5] V.E. Denny, V.J. Jusionis, Effects of non-condensable gas and forced flow on laminar film condensation, Int. J. Heat Mass Transfer 15 (1972) 315–326.
[6] Seungmin Oh, Shripad T. Revankar, Experimental and theoretical investigation of film condensation with noncondensable gas, Int. J. Heat Mass Transfer 49 (2006) 2523–2534.
[7] B. Mazzarotta, E. Sebastiani, Process design of condensers for vapor mixtures in the presence of non-condensable gases, Can. J. Chem. Eng. 73 (1995) 456.
[8] A.P. Burdukov, N.S. Bufetov, Experimental study of the absorption of water vapour by thin films of aqueous lithium bromide, Heat Trans.-Soviet Res. 12 (1980) 118–123.
[9] F. Cosenza, G.C. Vliet, Absorption in falling water/LiBr films on horizontal tubes, ASHRAE Trans. 96 (1990) 693–701.
[10] H.M. Sabir, I.W. Eames, Performance of film absorbers under the effect of a contaminant non-absorbable gas, Appl. Energy 63 (1999) 255–267.
[11] L.I. Heifets, D.M. Predtechenskaya, Yu.V. Pavlov, B.N. Okunev, Modeling of the dynamic effects in the adsorbent beds. 1. Simple method of estimation of thermal conductivity of the composite adsorbent bed ($CaCl_2$ impregnated into pores of silica gel lattice), Vestnik MGU Ser2 47 (4) (2006) 274–277.
[12] M.A. Lambert, Design of solar powered adsorption heat pump with ice storage, Appl. Therm. Eng. 27 (2007) 1612–1628.
[13] Yu.I. Aristov, B. Dawoud, I.S. Glaznev, A. Elyas, A new methodology of studying the dynamics of water vapor sorption/desorption under real operating conditions of adsorption heat pumps: experiment, Int. J. Heat Mass Transfer, doi:10.1016/j.ijheatmasstransfer.2007.10.042.
[14] B.N. Okunev, A.P. Gromov, L.I. Heifets, Yu.I. Aristov, A new methodology of studying the dynamics of water sorption/desorption under real operating conditions of adsorption heat pumps: modeling of coupled heat and mass transfer, Int. J. Heat Mass Transfer 51 (2008) 246–252.
[15] Yu.I. Aristov, M.M. Tokarev, G. Cacciola, G. Restuccia, Selective water sorbents for multiple applications: 1. $CaCl_2$ confined in mesopores of the silica gel: sorption properties, React. Kinet. Catal. Lett. 59 (2) (1996) 325–334.
[16] Yu.I. Aristov, G. Restuccia, G. Cacciola, V.N. Parmon, A family of new working materials for solid sorption air conditioning systems, Appl. Therm. Eng. 2 (2002) 191–204.
[17] G. Restuccia, A. Freni, S. Vasta, Yu.I. Aristov, Selective water sorbents for solid sorption chiller: experimental results and modelling, Int. J. Refrig. 27 (2004) 284–293.
[18] R. Lang, M. Roth, M. Stricker, Development of a modular zeolite–water heat pump, in: Proceedings of the International Sorption Heat Pump Conference, ISHPC 99, Munich, Germany, 1999, pp. 611–618.
[19] M. Medrano, M. Bourouis, H. Perez-Blanco, A. Coronas, A simple model for falling film absorption on vertical tubes in the presence of non-absorbables, Int. J. Refrig. 26 (2003) 108–116.